




Short Note

1,1'-[3,5-Bis((dodecyloxycarbonyl)-4-phenyl-1,4-dihydropyridine-2,6-diyl)bis(methylene)]bis[4-(anthracen-9-yl)pyridin-1-ium] Dibromide

Reinis Ozolins^{1,2}, Mara Plotniece², Karlis Pajuste¹, Reinis Putralis^{1,2}, Nadiia Pikun¹, Arkadij Sobolev¹, Aiva Plotniece^{1,2} and Martins Rucins^{1,*}

¹ Latvian Institute of Organic Synthesis, Aizkraukles 21, LV-1006 Riga, Latvia

² Department of Pharmaceutical Chemistry, Faculty of Pharmacy, Riga Stradiņš University, Dzirciema 16, LV-1007 Riga, Latvia

* Correspondence: rucins@osi.lv

Abstract: A synthesis of a cationic moiety and fluorescent moieties containing amphiphilic 1,4-dihydropyridine (1,4-DHP) derivatives was performed starting with the Hantzsch-type cyclization of dodecyl acetoacetate, phenylaldehyde and ammonium acetate. Bromination of the 2,6-dimethyl groups of a parent 1,4-DHP compound, followed by nucleophilic substitution of bromine with 4-(anthracen-9-yl)pyridine, produced the desired 1,1'-[3,5-bis((dodecyloxycarbonyl)-4-phenyl-1,4-dihydropyridine-2,6-diyl)bis(methylene)]bis[4-(anthracen-9-yl)pyridin-1-ium] dibromide. The obtained target compound was fully characterized by the IR, ¹H NMR, ¹³C NMR and HRMS data. Studies of the self-assembling properties and characterization of the nanoparticles obtained by the ethanol injection method were performed using dynamic light scattering (DLS) measurements. DLS measurement data showed that 1,1'-[3,5-bis((dodecyloxycarbonyl)-4-phenyl-1,4-dihydropyridine-2,6-diyl)bis(methylene)]bis[4-(anthracen-9-yl)pyridin-1-ium] dibromide produced liposomes that had average diameters of 200 nm when the samples were freshly prepared, and 140 nm after 7 days or 1 month storage. The PDI values of the samples were approximately 0.50 and their zeta-potential values were approximately 41 mV when the samples were freshly prepared, and 33 mV after storage. The obtained nanoparticles were stored at room temperature for one month and remained stable during that period. The mean molecular area of the cationic 1,4-DHP-anthracene hybrid **4** was 118 Å², while the mean molecular area of the cationic 1,4-DHP **5** without anthracene substituents was only 83 Å². The photoluminescence quantum yield (PLQY) value for the EtOH solution of the 1,4-DHP derivative **4** was 10.8%, but for the 1,4-DHP derivative **5** it was only 1.8%. These types of compounds could be used as synthetic lipids in the further development of prospective theranostic delivery systems.

Keywords: 1,4-dihydropyridine; pyridinium; anthracene; self-assembling properties; nanoparticles; DLS; fluorescent dyes; synthetic lipids



Citation: Ozolins, R.; Plotniece, M.; Pajuste, K.; Putralis, R.; Pikun, N.; Sobolev, A.; Plotniece, A.; Rucins, M. 1,1'-[3,5-Bis((dodecyloxycarbonyl)-4-phenyl-1,4-dihydropyridine-2,6-diyl)bis(methylene)]bis[4-(anthracen-9-yl)pyridin-1-ium] Dibromide. *Molbank* **2022**, *2022*, M1438. <https://doi.org/10.3390/M1438>

Academic Editor: Fawaz Aldabbagh

Received: 11 August 2022

Accepted: 31 August 2022

Published: 2 September 2022

Publisher's Note: MDPI stays neutral with regard to jurisdictional claims in published maps and institutional affiliations.



Copyright: © 2022 by the authors. Licensee MDPI, Basel, Switzerland. This article is an open access article distributed under the terms and conditions of the Creative Commons Attribution (CC BY) license (<https://creativecommons.org/licenses/by/4.0/>).

1. Introduction

Lipid nanoparticles were the first types of nanomedicines to be approved, and they are a well-studied class of nanocarriers for drug delivery. With the development of nanotechnologies, new efficient delivery systems have been proposed: mainly lipid-based nanosystems such as liposomes, solid lipid nanoparticles, nanostructured lipid carriers, monoolein aqueous dispersions, etc. [1–4]. A variety of nanoplatforms have been developed and applied to cancer therapy, imaging or their combination. Nanoplatforms with combined therapeutic and imaging functionalities display great potential, which has resulted in many encouraging advances in theranostics [5,6]. Fluorescent nanosystems mainly are formed as (1) probe-loaded, when the dye or probe is encapsulated into the

system during the formulation processes, and (2) labeled, when the probe or fluorescent moiety is covalently bound to the surface of the nanosystem [7].

Anthracene and anthracene derivatives have been extensively studied over the past few decades due to their photophysical, photochemical and biological properties [8]; heterocyclic compounds that are associated with anthracene moieties are potentially useful for various applications [9]. For example, an imidazole-anthracene hybrid molecule has shown polymorphism-dependent piezochromic fluorescence behavior [10], and pyridine containing fluorophores have excellent chemical, physical and good electron-transporting properties with strong fluorescence [11].

Among various heterocyclic systems, 1,4-dihydropyridine (1,4-DHP) derivatives serve as heterocyclic scaffolds due to their special features, such as their distinctive molecular structure, low molecular mass, and widespread pharmaceutical activities [12]. The 1,4-DHP derivatives depending on the molecule's architecture possess various biological activities. DHPs as multifunctional regulators have demonstrated not only cardiovascular activities, but also anticonvulsant, analgesic and memory-enhancing effects in the central nervous system. Due to regulatory action at the intracellular level, other properties, such as antibacterial, anticancer, hypoglycemic and antimutagenic properties, have also been found for 1,4-DHPs [13].

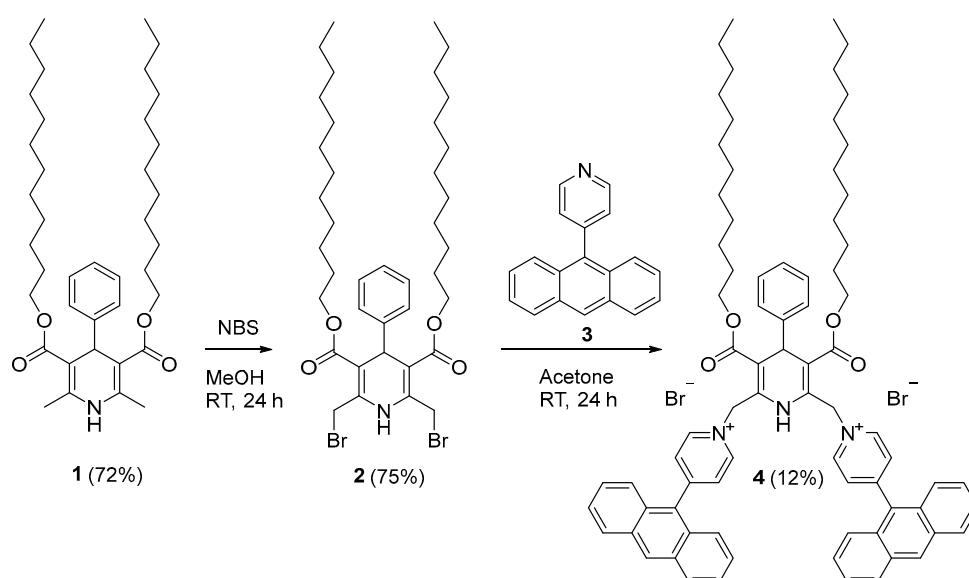
Derivatives of amphiphilic 1,4-DHP and related pyridine derivatives were studied as gene delivery systems [14–16]. These liposomes, which were filled by magnetic iron oxide nanoparticles, formed magnetoliposomes [17]. Magnetic nanoparticles functionalized by amphiphilic 1,4-DHP demonstrated bactericidal and immunomodulatory properties [18]. Insertion of an additional methylene group between the cationic moiety and the linker groups changes the delivery activity of 1,4-DHPs [19]. The amphiphilic 1,4-DHP possesses significant selective antiproliferative activity towards cancer cell lines HT-1080 and MH-22A; however, it still has very low activity in noncancerous NIH3T3 cells [20]. Propargyl group-derived 4-(N-alkylpyridinium)-1,4-DHP exhibits toxicity in Gram-positive and Gram-negative bacteria species and eukaryotic microorganisms [21], and it has also demonstrated calcium channel blocking and antioxidant activities [22]. Recently the synthesis and characterization of the physicochemical and self-assembling properties of cationic styrylpyridinium moieties derived from 4-(naphthalen-2-yl)-1,4-DHP have been demonstrated [23].

In this work, taking into account the fact that the introduction of an anthracene moiety as a fluorescent dye in a 1,4-DHP scaffold might form advanced hybrid structures possessing more pronounced fluorescence, synthesis of cationic amphiphilic 1,4-DHP was performed.

Herein, we report the synthesis and characterization of the physicochemical and self-assembling properties of a new original synthetic lipid-like compound—1,1'-[3,5-bis((dodecyloxycarbonyl)-4-phenyl-1,4-dihydropyridine-2,6-diyl)]bis-(methylene))bis[4-(anthracen-9-yl)pyridin-1-ium] dibromide. The evaluation of the self-assembling properties of the target amphiphilic 1,4-DHP **4** and the characterization of the formed nanoparticles were performed by dynamic light scattering (DLS) measurements in an aqueous solution. The nanoparticles were prepared by the ethanol injection method [24].

2. Results and Discussion

Taking into account the fact that the introduction of an anthracene moiety as a fluorescent dye in the synthetic cationic lipid structure might lead to the formation of original delivery systems with more pronounced fluorescent properties, synthesis of 1,1'-[3,5-bis((dodecyloxycarbonyl)-4-phenyl-1,4-dihydropyridine-2,6-diyl)]bis-(methylene))bis[4-(anthracen-9-yl)pyridin-1-ium] dibromide **4** was performed. 1,4-DHP-anthracene hybrid **4** was synthesized via a three step procedure. The synthetic process and the structures of all compounds are depicted in Scheme 1.



Scheme 1. Synthesis of 1,1'-[[3,5-bis((dodecyloxycarbonyl)-4-phenyl-1,4-dihydropyridine-2,6-diyl)bis-(methylene)]bis[4-(anthracen-9-yl)pyridin-1-ium] dibromide 4.

Firstly, a parent didodecyl 2,6-dimethyl-4-(naphthalen-2-yl)-1,4-dihydropyridine-3,5-dicarboxylate **1** was synthesized in a three-component Hantzsch-type reaction of dodecyl acetoacetate, benzaldehyde and ammonia in ethanol under reflux with a yield of 72% [15]. Bromination of the 2,6-methyl groups at the 1,4-DHP **1** was performed by N-bromosuccinimide (NBS), similarly to a previously described procedure [25]. A solution of NBS in methanol was added dropwise to a solution of 2,6-dimethyl-1,4-DHP **1** in methanol, the reaction mixture was stirred at r. t. for 2 h and the completion of the reaction mixture was monitored by TLC. The desired 2,6-bis(bromomethyl)-1,4-DHP **2** was obtained with a yield of 75%. The last step—nucleophilic substitution of bromine with 4-(anthracen-9-yl)pyridine (**3**)—was performed in acetone by stirring the reaction mixture at room temperature for 24 h; this step gave the target 1,1'-[[3,5-bis((dodecyloxycarbonyl)-4-phenyl-1,4-dihydropyridine-2,6-diyl)bis-(methylene)]bis[4-(anthracen-9-yl)pyridin-1-ium] dibromide (**4**) a 12% yield. 4-(Anthracen-9-yl)pyridine (**3**) was produced according to a previously published procedure, from 9-bromoanthracene and 4-pyridineboronic acid hydrate in a THF/H₂O (2:1) solution in the presence of K₂CO₃ and Pd(PPh₃)₄ [26].

The structures of compounds **1**, **2** [27] and **3** [26] were confirmed by the ¹H NMR spectra, which were in agreement with the data in the literature. The structure of the original compound **4** was established and confirmed on the base of the ¹H, ¹³C NMR, IR and HRMS data (Figures S1–S3, Supplementary Materials).

The ¹H NMR spectrum of the 1,4-DHP-anthracene hybrid **4** showed characteristic signals for 1,4-DHP 4-H and NH protons at 5.15 and 10.60 ppm, respectively. Characteristic AB-system signals from the 2,6-methylene protons were observed in the ¹H NMR spectrum at 5.89 and 6.39 ppm, and *para*-substituted pyridinium system signals were observed as two doublets at 8.30 and 9.32 ppm.

In the IR spectra, compound **4** demonstrated characteristic absorption bands above 3400 cm⁻¹ of the NH group and absorptions in 1700–1600 cm⁻¹ of its C=O and C=C groups.

Self-assembling properties are characteristic features of synthetic lipid-like compounds, including cationic moieties containing 1,4-DHPs. The hydrodynamic average diameter (*Z*_{av}), polydispersity index (PDI), zeta-potential (*Z*_{pot}) and stability of a nanoparticle formed by a 1,4-DHP-anthracene hybrid **4** in an aqueous medium were determined by the DLS method. Nanoparticles were prepared by the ethanol injection method, which involved the dissolution of a lipid-like compound into an organic solvent followed by dispersion of the lipid solution into water. This method was rapid, simple and easy to scale up [24]. The results are summarized in Table 1. The DLS measurements were performed on the

freshly prepared samples (entry 1, Table 1) and after the samples had been stored at room temperature for 7 (entry 2, Table 1) and 30 days (entry 3, Table 1).

Table 1. Values for the polydispersity indexes (PDI), Z-average (Z_{av}) diameters, diameters of the populations (D) as percentages (%) and zeta-potentials (Z_{pot}) of nanoparticles formed by 1,1'-[[3,5-bis((dodecyloxycarbonyl)-4-phenyl-1,4-dihydropyridine-2,6-diyl)bis-(methylene))bis[4-(anthracen-9-yl)pyridin-1-ium] dibromide (**4**) at a concentration of 0.1 mM in an aqueous solution obtained by DLS measurements. The PDI value describes the polydispersity of a sample; the D of a population shows the size of each fraction of nanoparticles (%), the Z_{av} diameter represents the average hydrodynamic diameter of all nanoparticles in the sample and the Z_{pot} value gives information about the surface charge of the nanoparticles.

| Entry | Condition, Days | Z_{av} D_H , nm | PDI | D, nm (%) | Z_{pot} , mV |
|-------|-----------------|---------------------|-------------|--------------------------|----------------|
| 1 | 0 * | 225 ± 4.0 | 0.51 ± 0.02 | 346 (87); 49 (9); 12 (4) | 41.6 ± 3.2 |
| 2 | 7 ** | 141 ± 3.0 | 0.49 ± 0.03 | 244 (90); 27 (10) | 34.5 ± 3.5 |
| 3 | 30 *** | 135 ± 3.0 | 0.47 ± 0.01 | 209 (90); 23 (10) | 32.8 ± 1.8 |

* Freshly prepared sample; ** after sample had been stored for 7 days at r. t.; *** after sample had been stored for 30 days at r. t.

It was demonstrated that a cationic 1,4-DHP-anthracene hybrid **4** in an aqueous medium formed nanoparticles with an average diameter of ~225 nm when the samples were freshly prepared, but the diameter decreased after 7 and 30 days of storage to ~141 and 135 nm, respectively. Values for the PDI confirmed that the samples possessed average homogeneity; thus, the PDI value for the freshly prepared samples was 0.51, after having been stored for 7 days the PDI value of the samples was 0.49, but after storage for 30 days the PDI value of the samples was 0.47. This could also be confirmed by the nanoparticle population ratio. Thus, all samples contained nanoparticle populations with size ratios of ~90/10%: 346/49, 244/27 and 209/23 nm for the freshly prepared samples and after 7 and 30 days of storage, respectively. Values for the zeta-potential of the nanoparticles formed by compound **4** indicated the positive surface charge, and the values were ~40 mV for the freshly prepared samples and ~33 nm for the samples after storage. According to the data in literature, the obtained zeta-potentials over ±20 mV confirmed that the formed nanoparticle solutions were also relatively electrostatically stable [28]. The DLS measurement of the mentioned sample was also performed after the sample had been stored for 3 months at room temperature, but an aggregation of nanoparticles occurred.

The substituents of the amphiphilic 1,4-DHP ring influence its ability to form nanoparticles, which could be observed in the examples of nanoparticles formed by the structurally related compounds that have been previously reported by us. Thus, 1,1'-[(3,5-bisdodecyloxycarbonyl-4-phenyl-1,4-dihydropyridine-2,6-diyl)dimethylen]bis(pyridin-1-ium) dibromide (**5**) formed particles with an average diameter of 110 nm and a PDI value 0.345 [15], which were stable for at least 3 months [29]. While 1,1'-[[3,5-bis(dodecyloxycarbonyl)-4-(thiophen-3-yl)-1,4-dihydropyridine-2,6-diyl]bis-(methylene)]bis(pyridin-1-ium) dibromide formed particles with an average diameter of approximately 80 nm and a PDI value of 0.399 for the freshly prepared samples, which were stable only for 1 week [30], and 1,1'-[[3,5-bis(dodecyloxycarbonyl)-4-(naphthalen-2-yl)-1,4-dihydropyridine-2,6-diyl]bis(methylene)]bis[4-[(E)-2-(naphthalen-2-yl)vinyl]pyridin-1-ium] dibromide formed particles with an average diameter of approximately 300 nm and a PDI value of 0.491 for the freshly prepared samples, which were also only stable for 1 week [23].

The amphiphilic 1,4-DHP derivative **4**, however, contained anthracene moieties, which are fluorophores, and the photoluminescence quantum yields (PLQY) were measured for comp. **4** and the structurally related 1,4-DHP amphiphile **5**, which did not contain any anthracene substituents. Structures of the compounds are depicted in Figure 1. The PLQY value for the EtOH solution of the 1,4-DHP-anthracene hybrid **4** was 10.8%, while for the EtOH solution of the 1,4-DHP derivative **5** it was only 1.8%. In addition, a visual comparison of the fluorescence of the ethanol solutions of compounds **5** and **4** under 365 nm light are shown in Figure 1.

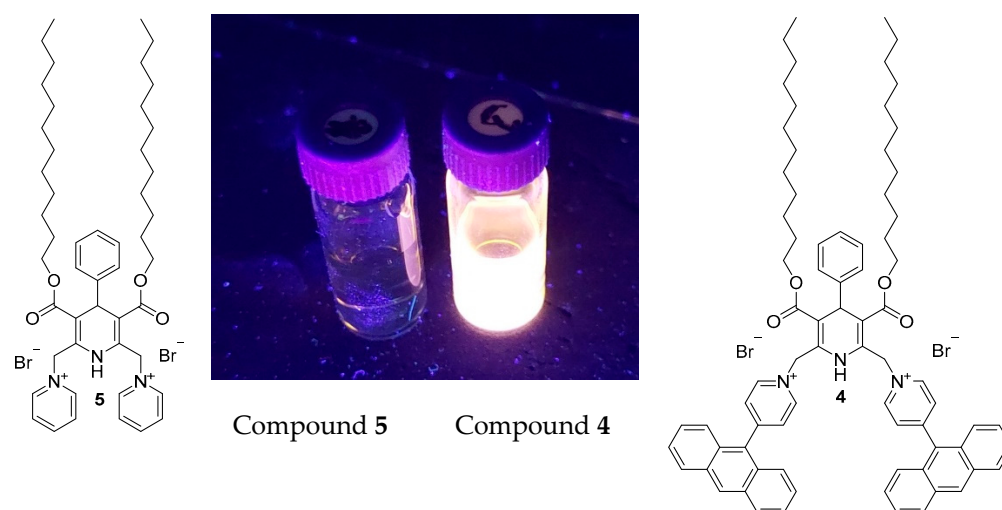


Figure 1. Structures and a visual comparison of the fluorescence of the ethanol solutions of compounds **5** and **4** under 365 nm light.

The properties of the monolayers composed of 1,4-DHP amphiphiles and their polar head areas were determined from π -A isotherms, which were obtained using the Langmuir-Blodgett trough (Figures S4–S6, Supplementary Materials), and calculated using previously published procedures [17]. A newly obtained cationic 1,4-DHP-anthracene hybrid **4** and a structurally related 1,4-DHP amphiphile **5** without anthracene substituents were chosen for this study. The critical surface pressure was defined as the surface pressure at which the monolayer collapsed. The mean molecular areas (MMA) of the compound of interest could be extracted from the π -A isotherms in the condensed liquid phase, and the obtained values for compounds **4** and **5** are listed in Table 2. The mechanical properties of the monolayer of compound **4** (entry 1, Table 2), compound **5** (entry 2, Table 2) and the data in the literature for compound **5** (entry 3, Table 2) can be found in Table 2.

Table 2. Mechanical properties of monolayers composed of 1,4-DHP amphiphiles **4** and **5** obtained using the Langmuir-Blodgett trough. P (mN/m) is the critical pressure of the monolayers; C_s^{-1} (mN/m) is the compressibility modulus; MMA (\AA^2) is the mean molecular area.

| Entry | Compound | P , mN/m | C_s^{-1} , mN/m | MMA, \AA^2 |
|-------|------------|------------------|-------------------|---------------------|
| 1 | 4 | 51.24 ± 0.49 | 100.99 ± 8.84 | 117.53 ± 3.65 |
| 2 | 5 | 45.28 ± 0.65 | 87.20 ± 8.84 | 88.72 ± 2.14 |
| 3 | 5 * | 46.62 ± 0.02 | 15.65 ± 1.24 | 82.77 ± 0.60 |

* Data from previous studies [17].

It was demonstrated that the mean molecular area of the cationic 1,4-DHP-anthracene hybrid **4** was 118\AA^2 , while the mean molecular area of the cationic 1,4-DHP **5** without anthracene substituents was only 83\AA^2 . Data for cationic 1,4-DHP **5** were in agreement with those that had been previously published [17].

3. Materials and Methods

3.1. General

All reagents were purchased from Acros Organics (Geel, Belgium), Sigma-Aldrich/Merck KGaA (Darmstadt, Germany) or Alfa Aesar (Lancashire, UK) and used without further purification. TLC was performed on silica gel 60 F₂₅₄ aluminium sheets 20 cm \times 20 cm (Merck KGaA, Darmstadt, Germany). Melting points were recorded on an OptiMelt digital melting point apparatus (Stanford Research Systems, Sunnyvale, CA, USA) and were uncorrected. ^1H and ^{13}C NMR spectra were recorded on a Bruker Avance Neo 400 MHz (Bruker Biospin GmbH, Rheinstetten, Germany). Chemical shifts in the hydrogen and

carbon atoms were presented in parts per million (ppm) and referred to the residual signals of the undeuterated DMSO- d_6 . Chemical shifts in the hydrogen and carbon atoms were presented in parts per million (ppm) and referred to the residual signals of the undeuterated DMSO- d_6 solvent (δ : 2.50) for the ^1H NMR spectra and (δ : 39.52) for the ^{13}C NMR spectra, respectively. Coupling constants J were reported in hertz (Hz). High resolution mass spectra (HRMS) were determined on an Acquity UPLC H-Class system (Waters, Milford, MA, USA) connected to a Waters Synapt GII Q-ToF operating in the ESI positive or negative ion mode on a Waters Acquity UPLC[®] BEH C18 column (1.7 μm , 2.1 mm \times 50 mm, using gradient elution with acetonitrile (0.1% formic acid) in water (0.1% formic acid). Infrared spectra were recorded with a Prestige-21 FTIR spectrometer (Shimadzu, Kyoto, Japan). The DLS measurements of the nanoparticles in the aqueous solution were carried out on a Zetasizer Nano ZSP (Malvern Panalytical Ltd., Malvern, UK) instrument with Malvern Instruments Ltd. Software 8.01.4906.

3.2. Synthesis of 1,1'-[3,5-Bis((dodecyloxycarbonyl)-4-phenyl-1,4-dihydropyridine-2,6-diyl)bis(methylene)]bis[4-(anthracen-9-yl)pyridin-1-ium] Dibromide (**4**)

To a solution of didodecyl 2,6-bis(bromomethyl)-4-phenyl-1,4-dihydropyridine-3,5-dicarboxylate, (**2**, 150 mg, 0.196 mmol) in acetone (10 mL) 4-(anthracen-9-yl)pyridine (**3**, 100 mg, 0.390 mmol) was added at r. t. and the resulting mixture was stirred at r. t. for 24 h. The precipitates were filtered off, washed with cold acetone and dried under vacuum conditions to give product **4** as a pale yellow powder (29 mg, 12%) with a melting point in the 160–162 $^\circ\text{C}$ range. IR ν_{max} (film) 3436, 2923, 2854, 1733, 1671, 1652, 1601 cm^{-1} . ^1H NMR (400 MHz, DMSO- d_6) δ : 10.60 (s, 1H), 9.32 (d, J = 6.4 Hz, 4H), 8.79 (s, 2H), 8.30 (d, J = 6.4 Hz, 4H), 8.15 (d, J = 8.5 Hz, 4H), 7.47–7.29 (m, 17H), 6.39 (AB-system, J = 14.7 Hz, 2H), 5.89 (AB-system, J = 14.7 Hz, 2H), 5.15 (s, 1H), 4.15–4.04 (m, 4H), 1.61–1.51 (m, 4H), 1.27–1.19 (m, 36H), 0.84 (t, J = 6.7 Hz, 6H) ppm. ^{13}C NMR (101 MHz, DMSO- d_6) δ : 165.9; 156.5; 145.8; 145.0; 138.7; 130.4; 129.6; 129.3; 128.8; 128.4; 128.2; 127.7; 127.1; 125.6; 124.4; 108.4; 64.6; 57.4; 31.3; 31.2; 29.1; 29.05; 29.03; 29.01; 28.8; 28.75; 28.72; 28.1; 25.6; 22.1; 13.9 ppm. HRMS TOF ES+ of $[\text{C}_{77}\text{H}_{86}\text{N}_3\text{O}_4 + \text{H}]^+$ (m/z) 1116.6618; calcd: 1116.6642.

3.3. Self-Assembling Properties of Compound **4** Using Dynamic Light Scattering Measurements

Samples for the DLS studies were prepared by making a stock solution of compound **4** in EtOH at a concentration of 1 mM. A stock solution of compound **4** (300 μL , 1 mM in EtOH 96%) was injected into 2.7 mL of deionized water with maximum stirring (IKA Vortex 2 (IKA, Staufen, Germany)) to give a sample with a final concentration of the compound of 0.1 mM. The sample was sonicated for 60 min at 60 $^\circ\text{C}$ using a bath-type sonicator (Cole Parmer Ultrasonic Cleaner 8891CPX (Vernon Hills, IL, USA)).

The DLS measurements of the nanoparticles in the aqueous solution were carried out on a Zetasizer Nano ZSP (Malvern Panalytical Ltd., Malvern, UK) instrument with Malvern Instruments Ltd. Software 8.01.4906, using the following specifications—medium: water; refractive index: 1.33; viscosity: 0.8872 cP; temperature: 25 $^\circ\text{C}$; dielectric constant: 78.5; nanoparticles: liposomes; refractive index of materials: 1.60; detection angle: 173 $^\circ$; wavelength: 633 nm. Data were analyzed using the multimodal number distribution software that was included with the instrument. The measurements were performed in triplicate in order to check their reproducibility.

3.4. Photoluminescence Measurements

Photoluminescence quantum yields (PLQY) were measured using a standard complementary integrating sphere (the measurement module contained a 150 mm inner diameter integrating sphere for the measurement of fluorescence quantum yields by the absolute method and reflection measurements).

3.5. Characterization of Monolayers Formed by 1,4-DHP Amphiphiles or Surface Pressure–Area (p – A) Isotherms

The surface pressure–molecular area (π – A) compression isotherms were measured using a computer-controlled Langmuir trough (Medium trough, KSV NIMA Instruments, Espoo, Finland; $A_{\text{total}} = 243 \text{ cm}^{-2}$) made of Teflon and equipped with two compression barriers. The surface pressure of the monolayer was monitored with a Wilhelmy plate made of platinum, which was cleaned by flushing it with ethanol and Milli-Q water and then burned by a Bunsen burner. Prior to the measurements, the trough and barriers were thoroughly rinsed with ethanol and Milli-Q water. The cleanliness of the aqueous surface was ensured by sweeping the barriers across the surface, and the aqueous surface was considered clean when $\pi \leq 0.1 \text{ mN/m}$. Monolayers were formed by carefully spreading an appropriate volume of the lipid solution in chloroform dropwise on the deionized water surface at $23 \text{ }^{\circ}\text{C}$ using a Hamilton microsyringe. The carrying solvent (CHCl_3) was allowed to evaporate for 10 min before compression began. The monolayers were compressed at a constant rate of 10 mm/min . Measurements were made at $23 \text{ }^{\circ}\text{C}$ and repeated at least three times to ensure the reproducibility of the results. The experimentally detected standard deviations of the molecular area and surface pressure did not exceed 2%.

3.6. Statistical Analysis

Results were expressed as mean standard deviations (SDs). All of the experiments were performed in triplicate.

4. Conclusions

Synthesis of the cationic 1,4-DHP-antrachene hybrid **4** was carried out via a multistep procedure. The compound was characterized by IR, ^1H NMR, ^{13}C NMR and HRMS data. DLS measurements confirmed that the cationic 1,4-DHP **4** in an aqueous solution formed nanoparticles with average homogeneity, with a PDI value of ~ 0.5 , an average diameter of 225 nm for the freshly prepared samples and $\sim 140 \text{ nm}$ after they had been stored. The value for the zeta-potential of the nanoparticles formed by compound **4** indicated a positive surface charge. The mean molecular area of the cationic 1,4-DHP derivative **4** was 118 \AA^2 , while the mean molecular area of the similar cationic 1,4-DHP **5** without anthracene substituents was only 83 \AA^2 . The photoluminescence quantum yield (PLQY) value for the EtOH solution of 1,4-DHP amphiphile **4** was 10.8%, which was six times higher than that of the 1,4-DHP amphiphile **5**, where the PLQY value was only 1.8%. These types of compounds could be used as synthetic lipids for the further development of prospective theranostic delivery systems.

Supplementary Materials: ^1H NMR (Figure S1), ^{13}C NMR (Figure S2) and HRMS spectra of compound **4** (Figure S3), surface pressure—mean molecular area isotherms (Figure S4) and compressibility modulus–surface pressure dependences graphs of compounds **4** (Figure S6) and **5** (Figure S5).

Author Contributions: Conceptualization was conducted by M.R. and A.P.; methodology and experimental works were conducted by R.O., R.P., N.P., M.P., K.P., A.S. and A.P.; data analysis, writing and editing of the paper were conducted by R.O., A.S., M.R., K.P. and A.P.; project administration and supervision were conducted by N.P., K.P., A.P. and M.R. All authors have read and agreed to the published version of the manuscript.

Funding: This research was funded by the EuroNanoMed3 Project NANO4GLIO No ES RTD/2020/9, the PostDocLatvia Project No 1.1.1.2/VIAA/2/18/373 (N.P.) and the PostDocLatvia Project No 1.1.1.2/VIAA/3/19/587 (K.P.).

Institutional Review Board Statement: Not applicable.

Informed Consent Statement: Not applicable.

Data Availability Statement: The data presented in this study are available in this article.

Acknowledgments: The authors are indebted to Marina Petrova for recording the NMR and IR spectra, to Solveiga Grinberga for the mass spectral analyses and to Kaspars Leduskrasts for the determination of quantum yields.

Conflicts of Interest: The authors declare no conflict of interest.

References

1. Sguizzato, M.; Esposito, E.; Cortesi, R. Lipid-based nanosystems as a tool to overcome skin barrier. *Int. J. Mol. Sci.* **2021**, *22*, 8319. [[CrossRef](#)] [[PubMed](#)]
2. Liu, P.; Chen, G.; Zhang, J. A Review of Liposomes as a Drug Delivery System: Current Status of Approved Products, Regulatory Environments, and Future Perspectives. *Molecules* **2022**, *27*, 1372. [[CrossRef](#)] [[PubMed](#)]
3. Mirgorodskaya, A.B.; Koroleva, M.Y.; Kushnazarova, R.A.; Mishchenko, E.V.; Petrov, K.A.; Lenina, O.A.; Vyshtakalyuk, A.B.; Voloshina, A.D.; Zakharova, L.Y. Microemulsions and nanoemulsions modified with cationic surfactants for improving the solubility and therapeutic efficacy of loaded drug indomethacin. *Nanotechnology* **2022**, *33*, 155103. [[CrossRef](#)] [[PubMed](#)]
4. Guimarães, D.; Cavaco-Paulo, A.; Nogueira, E. Design of liposomes as drug delivery system for therapeutic applications. *Int. J. Pharm.* **2021**, *601*, 120571. [[CrossRef](#)]
5. Tang, W.L.; Tang, W.H.; Li, S.D. Cancer theranostic applications of lipid-based nanoparticles. *Drug Discov. Today* **2018**, *23*, 1159–1166. [[CrossRef](#)]
6. Charron, D.M.; Chen, J.; Zheng, G. Theranostic lipid nanoparticles for cancer medicine. *Cancer Treat. Res.* **2015**, *166*, 103–127. [[CrossRef](#)]
7. Zingale, E.; Romeo, A.; Rizzo, S.; Cimino, C.; Bonaccorso, A.; Carbone, C.; Musumeci, T.; Pignatello, R. Fluorescent Nanosystems for Drug Tracking and Theranostics: Recent Applications in the Ocular Field. *Pharmaceutics* **2022**, *14*, 955. [[CrossRef](#)]
8. Baviera, G.S.; Donate, P.M. Recent advances in the syntheses of anthracene derivatives. *Beilstein J. Org. Chem.* **2021**, *17*, 2028–2050. [[CrossRef](#)] [[PubMed](#)]
9. Duraimurugan, K.; Harikrishnan, M.; Madhavan, J.; Siva, A.; Lee, S.J.; Theerthagiri, J.; Choi, M.Y. Anthracene-based fluorescent probe: Synthesis, characterization, aggregation-induced emission, mechanochromism, and sensing of nitroaromatics in aqueous media. *Environ. Res.* **2021**, *194*, 110741. [[CrossRef](#)]
10. Li, R.; Xiao, S.; Li, Y.; Lin, Q.; Zhang, R.; Zhao, J.; Yang, C.; Zou, K.; Li, D.; Yi, T. Polymorphism-dependent and piezochromic luminescence based on molecular packing of a conjugated molecule. *Chem. Sci.* **2014**, *5*, 3922–3928. [[CrossRef](#)]
11. Sun, Q.; Wang, H.; Xu, X.; Lu, Y.; Xue, S.; Zhang, H.; Yang, W. 9,10-Bis((Z)-2-phenyl-2-(pyridin-2-yl)vinyl)anthracene: Aggregation-induced emission, mechanochromic luminescence, and reversible volatile acids-amines switching. *Dye. Pigment.* **2018**, *149*, 407–414. [[CrossRef](#)]
12. Mathur, R.; Negi, K.S.; Shrivastava, R.; Nair, R. Recent developments in the nanomaterial-catalyzed green synthesis of structurally diverse 1,4-dihydropyridines. *RSC Adv.* **2021**, *11*, 1376–1393. [[CrossRef](#)] [[PubMed](#)]
13. Klusa, V. Atypical 1,4-dihydropyridine derivatives, an approach to neuroprotection and memory enhancement. *Pharmacol. Res.* **2016**, *113*, 754–759. [[CrossRef](#)] [[PubMed](#)]
14. Hyvönen, Z.; Plotniece, A.; Reine, I.; Chekavichus, B.; Duburs, G.; Urtti, A. Novel cationic amphiphilic 1,4-dihydropyridine derivatives for DNA delivery. *Biochim. Biophys. Acta-Biomembr.* **2000**, *1509*, 451–466. [[CrossRef](#)]
15. Pajuste, K.; Hyvonen, Z.; Petrichenko, O.; Kaldre, D.; Rucins, M.; Cekavicus, B.; Ose, V.; Skrivele, B.; Gosteva, M.; Morin-Picardat, E.; et al. Gene delivery agents possessing antiradical activity: Self-assembling cationic amphiphilic 1,4-dihydropyridine derivatives. *New J. Chem.* **2013**, *37*, 3062–3075. [[CrossRef](#)]
16. Petrichenko, O.; Rucins, M.; Vezane, A.; Timofejeva, I.; Sobolev, A.; Cekavicus, B.; Pajuste, K.; Plotniece, M.; Gosteva, M.; Kozlovska, T.; et al. Studies of the physicochemical and structural properties of self-assembling cationic pyridine derivatives as gene delivery agents. *Chem. Phys. Lipids* **2015**, *191*, 25–37. [[CrossRef](#)]
17. Petrichenko, O.; Plotniece, A.; Pajuste, K.; Rucins, M.; Dimitrijevs, P.; Sobolev, A.; Sprugis, E.; Cēbers, A. Evaluation of physicochemical properties of amphiphilic 1,4-dihydropyridines and preparation of magnetoliposomes. *Nanomaterials* **2021**, *11*, 593. [[CrossRef](#)]
18. Niemirowicz-Laskowska, K.; Głuszek, K.; Piktel, E.; Pajuste, K.; Durnaś, B.; Król, G.; Wilczewska, A.Z.; Janmey, P.A.; Plotniece, A.; Bucki, R. Bactericidal and immunomodulatory properties of magnetic nanoparticles functionalized by 1,4-dihydropyridines. *Int. J. Nanomed.* **2018**, *13*, 3411–3424. [[CrossRef](#)]
19. Apsite, G.; Timofejeva, I.; Vezane, A.; Vigante, B.; Rucins, M.; Sobolev, A.; Plotniece, M.; Pajuste, K.; Kozlovska, T.; Plotniece, A. Synthesis and comparative evaluation of novel cationic amphiphile C12-Man-Q as an efficient DNA delivery agent in vitro. *Molecules* **2018**, *23*, 1540. [[CrossRef](#)]
20. Rucins, M.; Smits, R.; Sipola, A.; Vigante, B.; Domracheva, I.; Turovska, B.; Muhamadejev, R.; Pajuste, K.; Plotniece, M.; Sobolev, A.; et al. Pleiotropic Properties of Amphiphilic Dihydropyridines, Dihydropyridones, and Aminovinylcarbonyl Compounds. *Oxid. Med. Cell. Longev.* **2020**, *2020*, 8413713. [[CrossRef](#)]
21. Rucins, M.; Dimitrijevs, P.; Pajuste, K.K.; Petrichenko, O.; Jackevica, L.; Gulbe, A.; Kibilda, S.; Smits, K.; Plotniece, M.; Tirzite, D.; et al. Contribution of Molecular Structure to Self-Assembling and Biological Properties of Bifunctional Lipid-Like 4-(N-Alkylpyridinium)-1,4-Dihydropyridines. *Pharmaceutics* **2019**, *11*, 115. [[CrossRef](#)] [[PubMed](#)]

22. Rucins, M.; Kaldre, D.; Pajuste, K.; Fernandes, M.A.S.; Vicente, J.A.F.; Klimaviciusa, L.; Jaschenko, E.; Kanepe-Lapsa, I.; Shestakova, I.; Plotniece, M.; et al. Synthesis and studies of calcium channel blocking and antioxidant activities of novel 4-pyridinium and/or N-propargyl substituted 1,4-dihydropyridine derivatives. *Comptes Rendus Chim.* **2014**, *17*, 69–80. [[CrossRef](#)]
23. Rucins, M.; Kaukulis, M.; Plotniece, A.; Pajuste, K.; Pikun, N.; Sobolev, A. 1,1'-[[3,5-Bis(dodecyloxycarbonyl)-4-(naphthalen-2-yl)-1,4-dihydropyridine-2,6-diyl]bis(methylene)]bis[4-[(E)-2-(naphthalen-2-yl)vinyl]pyridin-1-ium] dibromide. *Molbank* **2022**, *2022*, M1396. [[CrossRef](#)]
24. Charcosset, C.; Juban, A.; Valour, J.P.; Urbaniak, S.; Fessi, H. Preparation of liposomes at large scale using the ethanol injection method: Effect of scale-up and injection devices. *Chem. Eng. Res. Des.* **2015**, *94*, 508–515. [[CrossRef](#)]
25. Rucins, M.; Pajuste, K.; Sobolev, A.; Plotniece, M.; Pikun, N.; Pajuste, K.; Plotniece, A. Data for the synthesis and characterisation of 2,6-di(bromomethyl)-3,5-bis(alkoxycarbonyl)-4-aryl-1,4-dihydropyridines as important intermediates for synthesis of amphiphilic 1,4-dihydropyridines. *Data Br.* **2020**, *30*, 105532. [[CrossRef](#)]
26. Ramsay, W.J.; Szczypiński, F.T.; Weissman, H.; Ronson, T.K.; Smulders, M.M.J.; Rybtchinski, B.; Nitschke, J.R. Designed enclosure enables guest binding within the 4200 Å³ cavity of a self-assembled cube. *Angew. Chem.-Int. Ed.* **2015**, *54*, 5636–5640. [[CrossRef](#)]
27. Pajuste, K.; Plotniece, A.; Kore, K.; Intenberga, L.; Cekavicus, B.; Kaldre, D.; Duburs, G.; Sobolev, A. Use of pyridinium ionic liquids as catalysts for the synthesis of 3,5-bis(dodecyloxycarbonyl)-1,4-dihydropyridine derivative. *Cent. Eur. J. Chem.* **2011**, *9*, 143–148. [[CrossRef](#)]
28. Chibowski, E.; Szcześ, A. Zeta potential and surface charge of DPPC and DOPC liposomes in the presence of PLC enzyme. *Adsorption* **2016**, *22*, 755–765. [[CrossRef](#)]
29. Rucins, M.; Petricenko, O.; Pajuste, K.; Plotniece, M.; Pajuste, K.; Gosteva, M.; Cekavicus, B.; Sobolev, A.; Plotniece, A. Studies of Preparation and Stability of Liposomes Formed by 1,1'-[(3,5-Didodecyloxycarbonyl-4-phenyl-1,4-dihydropyridine-2,6-diyl)-dimethylen]bispyridinium Dibromide. *Adv. Mater. Res.* **2013**, *787*, 157–162. [[CrossRef](#)]
30. Rucins, M.; Pajuste, K.; Plotniece, A.; Pikun, N.; Rodik, R.; Vyshnevskiy, S.; Sobolev, A. Synthesis and Characterisation of 1,1'-[[3,5-Bis(dodecyloxy-carbonyl)-4-(thiophen-3-yl)-1,4-dihydropyridine-2,6-diyl]bis-(methylene)]bis(pyridin-1-ium) Dibromide. *Molbank* **2022**, *2022*, M1311. [[CrossRef](#)]